Acta Cryst E CRYSTALLOGRAPHIC COMMUNICATIONS

ISSN 2056-9890

N′-(1,3-Benzothiazol-2-yl)benzenesulfonohydrazide: crystal structure, Hirshfeld surface analysis and computational chemistry

Thomas C. Baddeley,[a] Marcus V. N. de Souza,[b] James L. Wardell,[a,c]‡ Mukesh M. Jotani[d] and Edward R. T. Tiekink[e]*

[a]Department of Chemistry, University of Aberdeen, Meston Walk, Old Aberdeen AB24 3UE, Scotland, [b]Instituto de Tecnologia em Fármacos e Farmanguinhos, Fundação Oswaldo Cruz, 21041-250 Rio de Janeiro, RJ, Brazil, [c]Instituto de Tecnologia em Fármacos Farmanguinhos, Fundação Oswaldo Cruz, 21041-250 Rio de Janeiro, RJ, Brazil, [d]Department of Physics, Bhavan's Sheth R. A. College of Science, Ahmedabad, Gujarat 380001, India, and [e]Research Centre for Crystalline Materials, School of Science and Technology, Sunway University, 47500 Bandar Sunway, Selangor Darul Ehsan, Malaysia. *Correspondence e-mail: edwardt@sunway.edu.my

Received 13 March 2019
Accepted 23 March 2019

Edited by W. T. A. Harrison, University of Aberdeen, Scotland

‡ Additional correspondence author, e-mail: j.wardell@abdn.ac.uk.

Keywords: crystal structure; benzothiazole; sulfonylhydrazinyl; hydrogen bonding; Hirshfeld surface analysis; computational chemistry.

CCDC reference: 1905136

Supporting information: this article has supporting information at journals.iucr.org/e

The asymmetric unit of the title compound, $C_{13}H_{11}N_3O_2S_2$, comprises two independent molecules (*A* and *B*); the crystal structure was determined by employing synchrotron radiation. The molecules exhibit essentially the same features with an almost planar benzothiazole ring (r.m.s. deviation = 0.026 and 0.009 Å for *A* and *B*, respectively), which forms an inclined dihedral angle with the phenyl ring [28.3 (3) and 29.1 (3)°, respectively]. A difference between the molecules is noted in a twist about the N—S bonds [the C—S—N—N torsion angles = −56.2 (5) and −68.8 (5)°, respectively], which leads to a minor difference in orientation of the phenyl rings. In the molecular packing, *A* and *B* are linked into a supramolecular dimer *via* pairwise hydrazinyl-N—H···N(thiazolyl) hydrogen bonds. Hydrazinyl-N—H···O(sulfonyl) hydrogen bonds between *A* molecules assemble the dimers into chains along the *a*-axis direction, while links between centrosymmetrically related *B* molecules, leading to eight-membered $\{\cdots HNSO\}_2$ synthons, link the molecules along [001]. The result is an undulating supramolecular layer. Layers stack along the *b*-axis direction with benzothiazole-C—H···O(sulfonyl) points of contact being evident. The analyses of the calculated Hirshfeld surfaces confirm the relevance of the above intermolecular interactions, but also serve to further differentiate the weaker intermolecular interactions formed by the independent molecules, such as π–π interactions. This is also highlighted in distinctive energy frameworks calculated for the individual molecules.

1. Chemical context

Benzothiazole derivatives have attracted attention over a long period of time because of their wide spectrum of biological activities and the benzothiazole framework remains today an important scaffold for the design and synthesis of active molecules (Gill *et al.*, 2015; Reshma *et al.*, 2017; Thakkar *et al.*, 2017; Dar *et al.*, 2016). Among recent reports on benzothiazole derivatives are those on 2-arylidenehydrazinylbenzothiazoles, which include anti-tumour activities (Lindgren *et al.*, 2014; Nogueira *et al.*, 2010; Katava *et al.*, 2017) and anti-tuberculosis activity against *M. tuberculosis* ATTC 27294 (Pinheiro *et al.*, 2019); crystal structure determinations have also been included in each of these studies. Less work has been carried out on other 2-hydrazinylbenzothiazoles, such as the arenesulfonyl derivatives, 2-(2-Ar-sulfonylhydrazinyl)-1,3-benzothiazoles. Only a brief report has appeared on their anti-

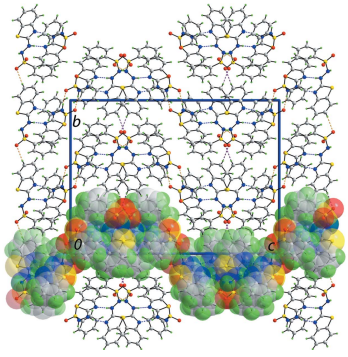

microbial activities (Rao *et al.*, 2004) and only very recently has a crystal structure determination of the species where Ar = 3-$O_2NC_6H_4$ has been described (Morscher *et al.*, 2018). Herein, as a continuation of the latter studies, the crystal and molecular structures of the title compound, (I), are described. The X-ray intensity data were collected on a small sample with synchrotron radiation and crystallography revealed the presence of two independent molecules in the asymmetric unit. In order to ascertain the individual contributions of these molecules to the molecular packing, an analysis of the calculated Hirshfeld surfaces was also conducted.

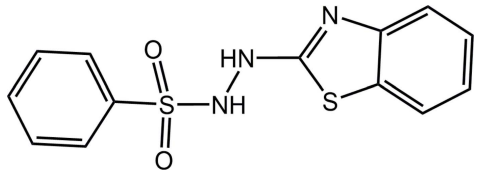

2. Structural commentary

Two independent molecules comprise the asymmetric unit of (I) and their molecular structures are shown in Fig. 1. In the S1-containing molecule, the r.m.s. deviation of the nine atoms forming the benzothiazole ring is 0.026 Å with maximum deviations out of the plane being 0.038 (8) Å for the C4 atom and 0.029 (6) Å for C2. The equivalent values for the S3-molecule are 0.009 Å with deviations of 0.010 (6) Å for the C16 atom and 0.013 (7) Å for C15. The dihedral angle between the benzothiazole and phenyl rings is 28.3 (3) and 29.1 (3)° for the S1- and S3-molecules, respectively, indicating very similar overall conformations for the molecules. This is reflected in the small r.m.s. bond and angle fits of 0.0196 Å and 1.126°, respectively (Spek, 2009). However, as seen from Fig. 2, the twist in the molecules about the N—S bonds differs, as seen in the disparity of about 12° in the C8—S2—N3—N2 [−56.2 (5)°] and C21—S4—N6—N5 [−68.8 (5)°] torsion angles. This leads to a lateral mismatch in the phenyl groups.

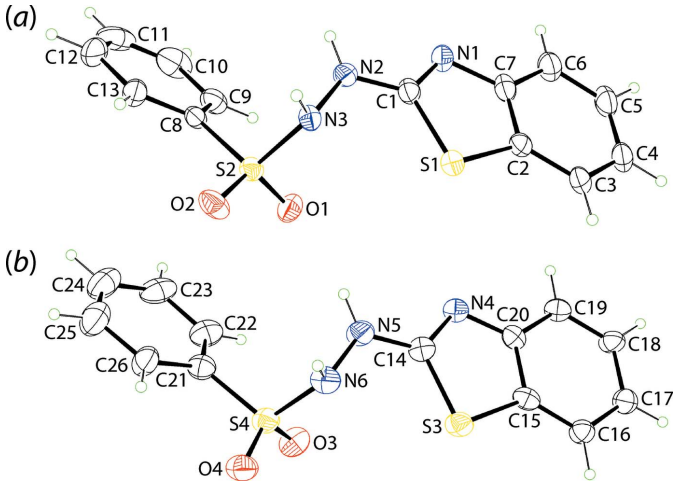

Figure 1
The molecular structures of the two independent molecules of (I), showing the atom-labelling scheme and displacement ellipsoids at the 25% probability level.

Table 1
Hydrogen-bond geometry (Å, °).

D—H···A	D—H	H···A	D···A	D—H···A
N2—H2*N*···N4	0.88 (4)	1.96 (4)	2.840 (7)	176 (8)
N3—H3*N*···O1^{i}	0.88 (3)	2.09 (4)	2.930 (7)	160 (5)
N5—H5*N*···N1	0.88 (5)	2.04 (4)	2.900 (7)	165 (6)
N6—H6*N*···O4^{ii}	0.89 (3)	2.07 (3)	2.956 (6)	175 (6)
C4—H4···O2^{iii}	0.95	2.55	3.450 (8)	159

Symmetry codes: (i) $x-\frac{1}{2}, y, -z+\frac{1}{2}$; (ii) $-x+1, -y+1, -z+1$; (iii) $-x+\frac{3}{2}, y-\frac{1}{2}, z$.

3. Supramolecular features

The molecular packing of (I) features hydrazinyl-N—H···N(thiazolyl) and hydrazinyl-N—H···O(sulfonyl) conventional hydrogen bonds, Table 1. The hydrazinyl-N—H···N(thiazolyl) hydrogen bonds serve to link the two molecules comprising the asymmetric unit into a dimeric aggregate *via* an eight-membered {···HNCN}$_2$ synthon, Fig. 3(*a*). Each of the remaining hydrazinyl-N—H atoms forms a hydrogen bond to a sulfonyl-O atom derived from a symmetry-related molecule. The hydrazinyl-N—H···O(sulfonyl) hydrogen bonds involving S1-molecules give rise to *C*(4), {···HNSO}$_n$, supramolecular chains along the *a*-axis direction. By contrast, those involving the S3-molecules occur between centrosymmetrically related molecules and lead to an eight-membered {···HNSO}$_2$ synthon. The latter serve to link molecules along the *c*-axis direction so that a supramolecular layer, with an undulating topology, in the *ac* plane results, Fig. 3(*b*). The distinctive modes of the hydrazinyl-N—H···O(sulfonyl) hydrogen bonds just outlined provide a clear differentiation between the molecules. The most obvious points of contact to link layers along the *b*-axis direction are of the type benzothiazole-C—H···O(sulfonyl), Table 1 and Fig. 3(*c*).

4. Hirshfeld surface analysis

The Hirshfeld surfaces calculated for (I) were performed following procedures outlined recently (Tan *et al.*, 2019) and provide additional information on the distinctive contributions made to the molecular packing by the independent molecules.

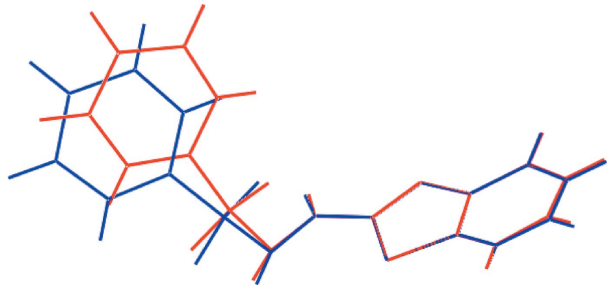

Figure 2
An overlay diagram of the S1-containing (red image) and S3-containing (blue) molecules. The molecules have been overlapped so the thiazole rings are coincident.

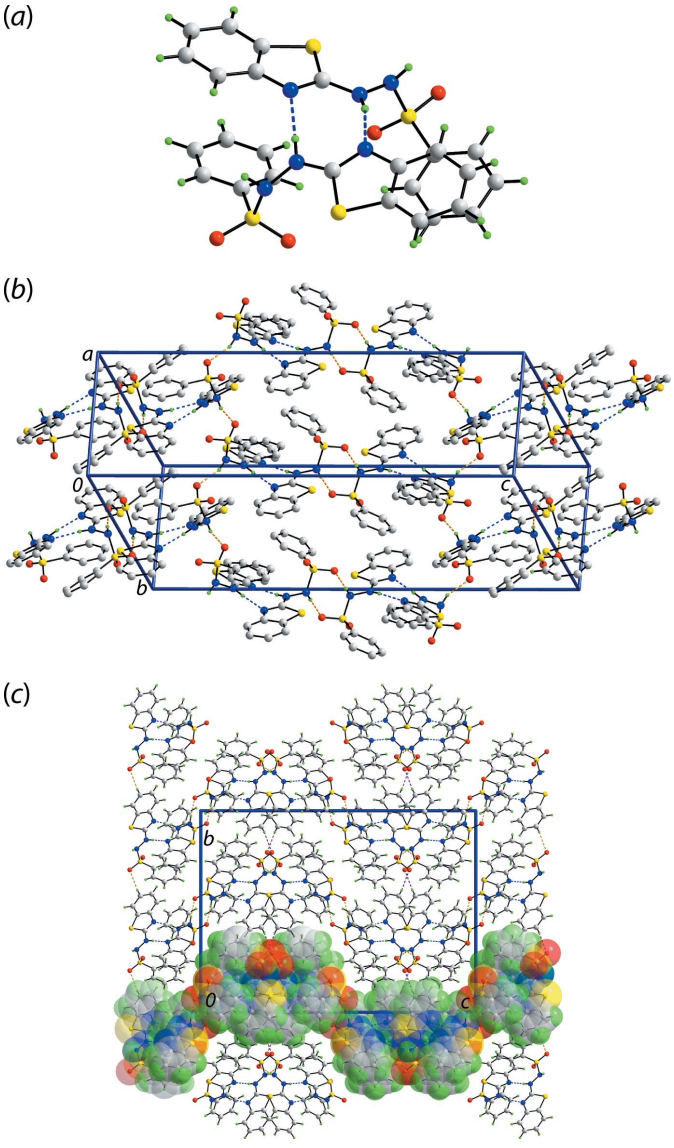

Figure 3
Supramolecular association in the crystal of (I): (*a*) dimeric aggregate sustained by hydrazide-N—H···N(thiazolyl) hydrogen bonds shown as blue dashed lines, (*b*) supramolecular layer in the *ac* plane whereby the dimers of (*a*) are linked by hydrazide-N—H···O(sulfonyl) hydrogen bonds (orange dashed) lines (non-acidic hydrogen atoms have been omitted) and (*c*) a view of the unit-cell contents shown in projection down the *a* axis. The benzothiazole-C—H···O(sulfonyl) interactions are shown as purple dashed lines and one layer has been highlighted in space-filling mode.

On the Hirshfeld surfaces mapped over d_{norm} for the S1-containing molecule, Fig. 4(*a*),(*b*), and the S3-molecule, Fig. 4(*c*),(*d*), the influence of the hydrazinyl-N—H···N(thiazolyl) hydrogen bonds sustaining the dimeric aggregate, Table 1, are evident as broad and bright-red spots near the participating atoms. The presence of intermolecular N—H···O hydrogen bonds involving the hydrazinyl-N3, N6 and sulfonyl-O1, O4 atoms are also viewed as broad and bright-red spots near the respective atoms in the images of Fig. 4. In addition, the weak C—H···O contacts are characterized by the diminutive red spots near the benzothiazolyl-H4 and sulfonyl-O2 atoms, Fig. 4(*b*), and the faint-red spots near the benzene-H11, benzothiazolyl-H19 and sulfonyl-O2,O4 atoms in Fig. 4(*a*)–(*c*). The presence of a short interatomic C···C contact involving atoms C20 and C23 of the S3-molecule, Table 2, describing π–π stacking interactions between symmetry-related S1-thiazole and benzene (C21–C26) rings is evident as the faint-red spots near these atoms in Fig. 4(*c*),(*d*).

Table 2
Summary of short interatomic contacts (Å) in (I).

Contact	Distance	Symmetry operation
H10···H16	2.17	$\frac{1}{2}+x, \frac{3}{2}-y, 1-z$
H11···O4	2.54	$-\frac{1}{2}+x, \frac{3}{2}-y, 1-z$
H19···O2	2.51	$-\frac{1}{2}+x, y, \frac{1}{2}-z$
C7···H3	2.78	$-\frac{1}{2}+x, y, \frac{1}{2}-z$
C20···C23	3.315 (10)	$-1+x, y, z$

The donors and acceptors of the N—H···N and N—H···O hydrogen bonds are also viewed as the intense-blue and -red regions corresponding to positive and negative electrostatic potentials on the Hirshfeld surfaces mapped over the calcu-

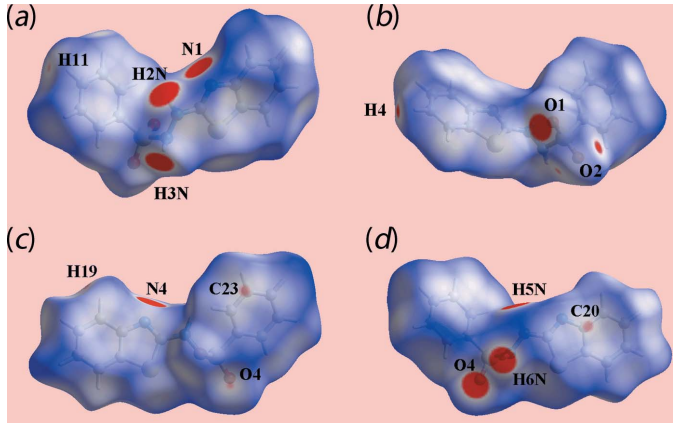

Figure 4
Views of the Hirshfeld surface for (I) mapped over d_{norm} for (*a*) and (*b*) the S1-containing molecule (range: − 0.120 to +1.433 arbitrary units) and (*c*) and (*d*) the S3-containing molecule (−0.120 to +1.392 arbitrary units).

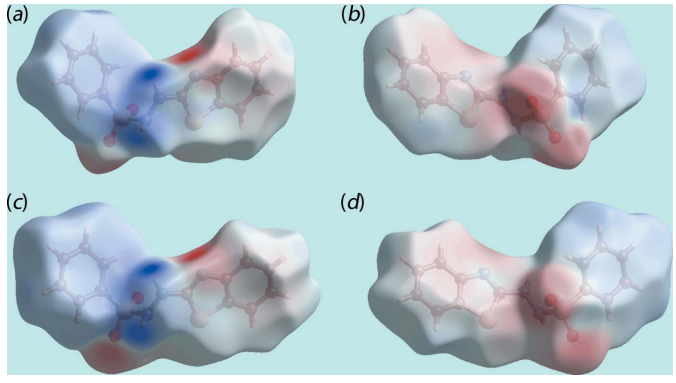

Figure 5
Views of the Hirshfeld surface for (I) mapped over the electrostatic potential for (*a*) and (*b*) the S1-containing molecule (range: −0.137 to +0.175 atomic units) and (*c*) and (*d*) the S3-containing molecule (−0.141 to +0.152 atomic units). The red and blue regions represent negative and positive electrostatic potentials, respectively.

Table 3
Summary of π–π contacts (Å) in (I).

Ring 1	Ring 2	Distance	Symmetry operation
Cg(C8–C13)	*Cg*(S3,C14,N4,C20–C15)	3.848 (4)	*x*, *y*, *z*
Cg(C8–C13)	*Cg*(C15–C20)	3.891 (5)	*x*, *y*, *z*
Cg(S3—C14—N4—C20—C15)	*Cg*(C21–C26)	3.923 (4)	−1 + *x*, *y*, *z*

lated electrostatic potentials for the S1- and S3-molecules in the images of Fig. 5.

An additional distinction in the molecular environments about the crystallographically independent molecules, over and above the hydrazinyl-N—H···O(sulfonyl) hydrogen bonds discussed above, is apparent in terms of their participation in π–π interactions, Table 3. Thus, the benzene and benzothiazole rings of the S3-molecule participate in such contacts in contrast to the involvement of only the benzene ring of the S1-molecule, as illustrated in Fig. 6(*a*). The influence of the short interatomic H···H contact between benzene-H10 (S1-molecule) and benzothiazolyl-H16 (S3-molecule) atoms is also illustrated in Fig. 6(*b*) through the red dashed lines superimposed on Hirshfeld surface mapped over the electrostatic potential.

The overall two-dimensional fingerprint plot for the individual S1-and S3-molecules, and entire (I) are shown in Fig. 7(*a*), and those delineated into H···H, O···H/H···O, S···H/H···S, C···H/H···C, N···H/H···N and C···C contacts

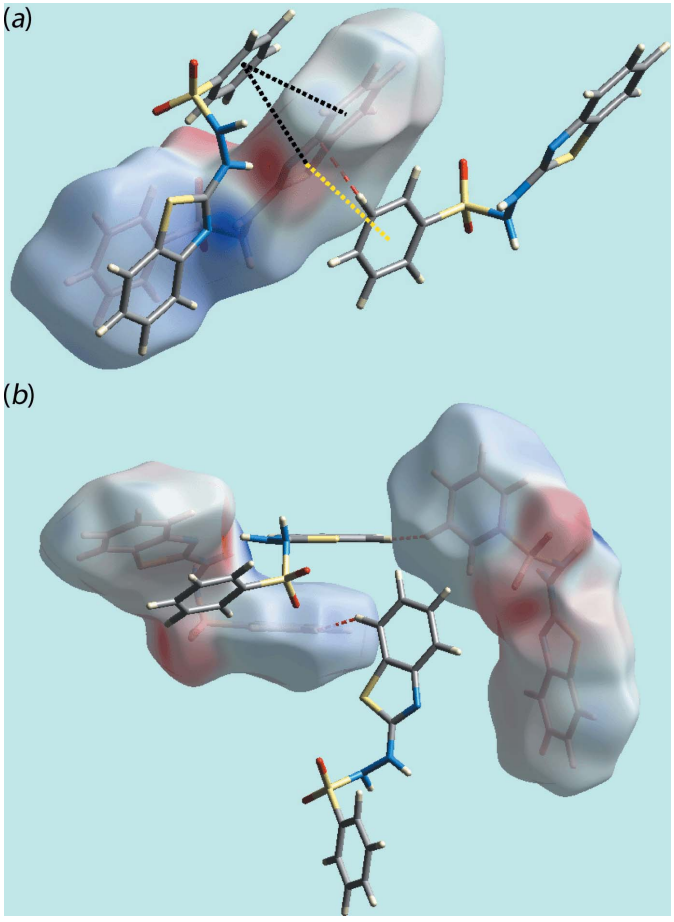

Figure 6
Views of Hirshfeld surfaces mapped over the electrostatic potential highlighting (*a*) π–π stacking between the molecules comprising the asymmetric unit (through black dotted lines) and between symmetry-related molecules (yellow) and short interatomic C···C contacts (red) and (*b*) short interatomic H···H contacts through red dashed lines.

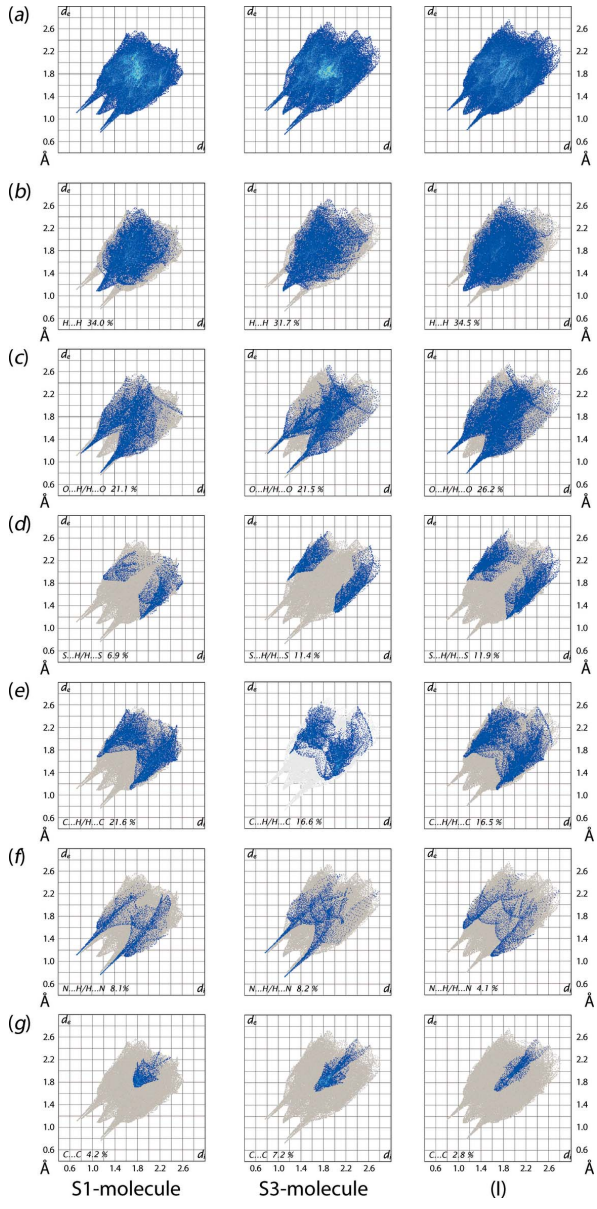

Figure 7
(*a*) The full two-dimensional fingerprint plot for the S1-molecule in (I), the S3-containing molecule and overall (I) and (*b*)–(*f*) those delineated into H···H, O···H/H···O, N···H/H···N, C···H/H···C, S···H/H···S and C···C contacts, respectively.

Table 4
Percentage contributions of interatomic contacts to the Hirshfeld surface for (I).

	Percentage contribution		
Contact	S1-molecule	S3-molecule	overall (I)
H···H	34.0	31.7	34.5
O···H/H···O	21.1	21.5	26.2
C···H/H···C	21.6	16.6	16.5
S···H/H···S	6.9	11.4	11.9
N···H/H···N	8.1	8.2	4.1
C···C	4.2	7.2	2.8
C···O/O···C	0.9	0.9	1.1
C···S/S···C	1.2	1.2	1.6
C···N/N···C	0.7	1.3	0.4
O···O	0.6	0.0	0.4
S···N/N···S	0.8	0.0	0.5

are illustrated in Fig. 7(*b*)–(*g*); the percentage contributions from different interatomic contacts to their respective Hirshfeld surfaces are quantitatively summarized in Table 4. Although the overall fingerprint plots for the S1- and S3-molecules in Fig. 7(*a*) are only slightly different, their delineated fingerprint plots in Fig. 7(*b*)–(*g*) clearly indicate their distinct modes of supramolecular association in the crystal.

The fingerprint plots delineated into H···H contacts for the S1- and S3-molecules in Fig. 7(*b*) represent the complementary pair of knife-edge tips at $d_e + d_i \sim 2.2$ Å which merge to form the conical tip in the respective plot for overall (I). The pair of spikes at $d_e + d_i \sim 2.0$ Å in the fingerprint plot delineated into O···H/H···O contacts for both independent molecules in Fig. 7(*c*), with nearly the same percentage contributions to the Hirshfeld surfaces (Table 4), arises owing to the involvement of the atoms of the respective molecules in the intermolecular N—H···O hydrogen bonds which finally superimpose in the plot for overall (I). In the fingerprint plot delineated into N···H/H···N contacts in Fig. 7(*f*), the pair of spikes at $d_e + d_i \sim 1.8$ Å and 1.9 Å for the S1- and S3-molecules, respectively, represent the presence of the N—H···N hydrogen bonds between them, to form the dimeric aggregate shown in Fig. 2(*a*). These features of the fingerprint plots disappear in the corresponding plot for overall (I) correlating with the decreased the percentage contribution from these contacts to the overall Hirshfeld surface (Table 4).

The presence of the short interatomic C···H contact between the atoms of S1-molecules result in the pair of peaks at $d_e + d_i \sim 2.8$ Å in the fingerprint plot delineated into C···H/H···C contacts in Fig. 7(*e*) for the S1-molecule and for overall (I). The fingerprint plots delineated into S···H/H···S contacts in the three images of Fig. 7(*d*) indicate the interatomic separations are greater than the sum of the van der Waals radii suggesting their limited influence on the molecular packing. The distinct, arrow-shaped distribution of points with different percentage contributions due to C···C contacts illustrated in Fig. 7(*g*) are due from the different π–π contacts made by the S1- and S3-molecules. The small contributions from the other interatomic contacts have negligible effects upon the molecular packing.

5. Computational chemistry

The pairwise interaction energies between the molecules in the crystal are calculated by summing up four energy components, comprising electrostatic (E_{ele}), polarization (E_{pol}), dispersion (E_{dis}) and exchange-repulsion (E_{rep}) (Turner *et al.*, 2017). The energies were obtained by using the wave function calculated at the B3LYP/6-31G(*d*,*p*) level of theory for each independent molecule. The individual energy components as well as total interaction energies relative to the respective reference molecule within the molecular cluster are illustrated in Fig. 8.

The strength and the nature of the intermolecular interactions in terms of their energies are quantitatively summarized in Table 5. The results reveal electrostatic interactions to be significant in the N—H···N hydrogen bonds which link the two independent molecules in the crystal *via* the $\{\cdots HNCN\}_2$ synthon. In the N—H···O hydrogen bond involving the S1-molecule, the electrostatic as well as dispersive components are dominant in contrast to a major contribution from only the electrostatic energy for the analogous hydrogen bond formed by the S3-molecule. This result is correlated with the latter hydrogen bonding linking S3-molecules *via* a $\{\cdots HNSO\}_2$ synthon as opposed to the chain sustained by the former. The weak intermolecular C—H···O interactions in the crystal have major contributions from dispersion energy components. It is also evident from the comparison of the total energies of the intermolecular interactions in Table 5 that the N—H···N hydrogen bonds between the molecules comprising the asymmetric unit are stronger than the N—H···O hydrogen bonds, and that the C—H···O contacts are significantly weaker than these.

The magnitudes of the intermolecular energies are represented graphically in the energy frameworks in Fig. 9. Here,

Table 5
Interaction energies (kJ mol^{-1}) for selected close contacts in (I).

contact	$E_{electrostatic}$	$E_{polarization}$	$E_{dispersion}$	$E_{exchange\text{-}repulsion}$	E_{total}
N2—H2*N*···N4	−121.4	−30.0	−81.2	158.8	−123.1
N5—H5*N*···N1	−121.4	−30.0	−81.2	158.8	−123.1
N3—H3*N*···O1^{i}	−39.3	−10.5	−40.0	52.1	−51.9
N6—H6*N*···O4^{ii}	−69.0	−15.7	−29.7	65.0	−70.3
C4—H4···O2^{iii}	−4.2	−1.3	−15.4	13.4	−10.6
C19—H19···O2^{i}	−1.0	−2.0	−14.8	11.6	−8.2
C11—H11···O4^{iv}	−10.2	−2.0	−7.6	6.8	−14.7

Symmetry codes: (i) $x-\frac{1}{2}, y, -z+\frac{1}{2}$; (ii) $-x+1, -y+1, -z+1$; (iii) $-x+\frac{3}{2}, y-\frac{1}{2}, z$; (iv) $x-\frac{1}{2}, -y+\frac{3}{2}, -z+1$

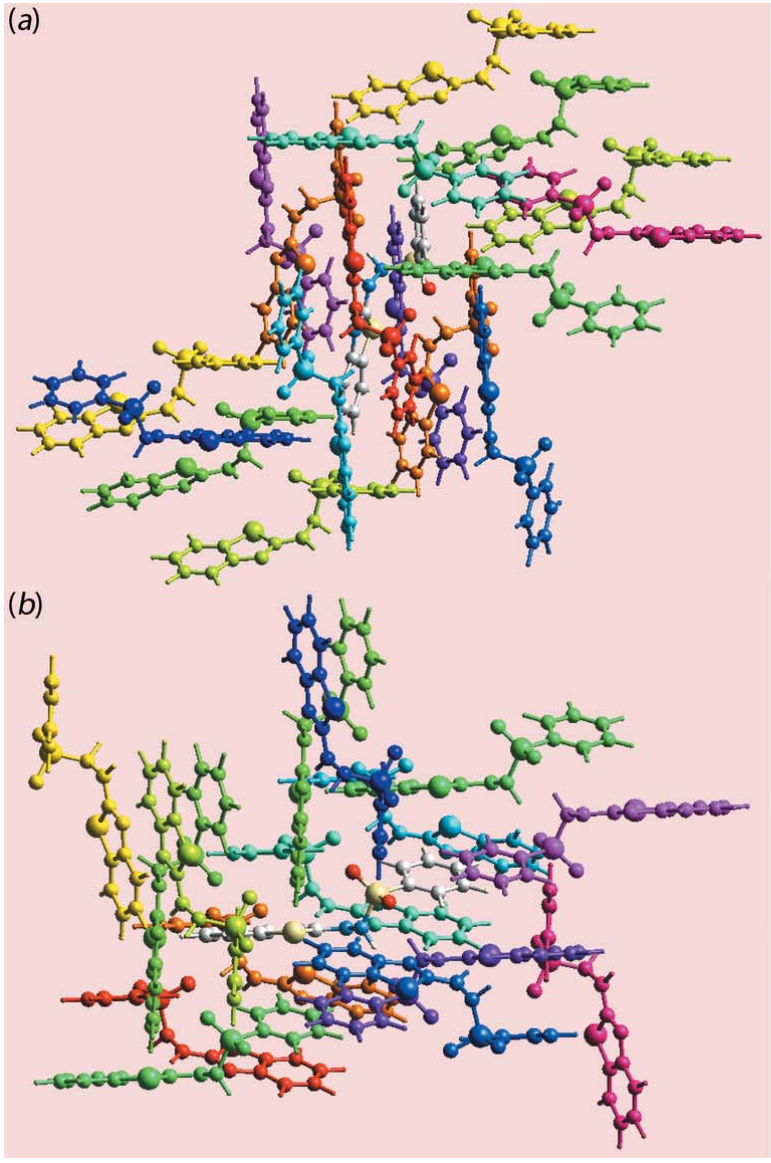

	N	Symmetry operation	R	E_{ele}	E_{pol}	E_{dis}	E_{rep}	E_{tot}
	1	-	3.93	-121.4	-30.0	-81.2	158.8	-123.1
	2	½ + x, y, ½ - z	5.52	-39.3	-10.5	-40.0	52.1	-51.9
	2	½ - x, ½ + y, z	11.97	-2.6	-0.5	-3.9	0.7	-6.2
	2	½ - x, ½ + y, z	11.47	-4.2	-1.3	-15.4	13.4	-10.6
	2	-x, ½ + y, ½ - z	11.32	1.9	-1.3	-9.2	3.6	-4.8
	1	-	9.75	1.7	-0.8	-7.0	4.6	-2.0
	1	-	10.55	-10.2	-2.0	-7.6	6.8	-14.7
	1	-	9.79	2.6	-0.4	-2.1	0.0	0.7
	1	-	8.87	-1.7	-1.9	-14.2	7.8	-10.8
	1	-	12.77	-1.3	-0.2	-7.8	6.7	-4.1
	1	-	7.90	-1.0	-2.0	-14.8	11.6	-8.2
	1	-	8.86	-3.8	-0.9	-7.0	5.2	-7.5
	1	-	11.85	0.7	-0.8	-7.9	3.4	-4.7

	N	Symmetry operation	R	E_{ele}	E_{pol}	E_{dis}	E_{rep}	E_{tot}
	1	-	8.87	-1.7	-1.9	-14.2	7.8	-10.8
	1	-	7.90	-1.0	-2.0	-14.8	11.6	-8.2
	1	-	12.77	-1.3	-0.2	-7.8	6.7	-4.1
	1	-	9.75	1.7	-0.8	-7.0	4.6	-2.0
	2	½ + x, ½ - y, - z	8.05	-0.3	-2.2	-11.8	6.9	-8.0
	2	x, y, z	8.91	-2.5	-2.6	-29.4	15.6	-20.6
	1	-	3.93	-121.4	-30.0	-81.2	158.8	-123.1
	1	-	8.86	-3.8	-0.9	-7.0	5.2	-7.5
	1	-	9.79	2.6	-0.4	-2.1	0.0	0.7
	1	-	10.55	-10.2	-2.0	-7.6	6.8	-14.7
	1	-x, -y, -z	6.79	-69.0	-15.7	-29.7	65.0	-70.3
	1	-x, -y, -z	12.08	-8.8	-1.4	-9.8	2.3	-17.5
	1	-	11.85	0.7	-0.8	-7.9	3.4	-4.7

Figure 8
The colour-coded interaction mapping for the clusters within 3.8 Å of the (*a*) S1-molecule and (*b*) S3-molecule.

the supramolecular architecture of the crystal is viewed through cylinders joining centroids of molecular pairs using red, green and blue colour codes for the energy components E_{ele}, E_{disp} and E_{tot}, respectively. The radius of the cylinder is proportional to the magnitude of the interaction energy which have been adjusted to the same scale factor within 2 × 2 × 2 unit cells. The illustrated energy frameworks constructed for clusters of both the independent molecules also indicate their participation in distinct modes of supramolecular association.

6. Database survey

As indicated in the *Chemical context*, the structure determination of (I) is only the second such analysis for 2-(2-Ar-sulfonylhydrazinyl)-1,3-benzothiazole molecules, the first being the example where Ar = 3-$O_2NC_6H_4$ (Morscher *et al.*, 2018); in (I), Ar = C_6H_5. In the literature precedent, there are also two independent, but conformationally similar molecules in the asymmetric unit and these, too, are linked into supramolecular dimers *via* hydrazinyl-N—H···N(thiazolyl) hydrogen bonds. As reported for the literature structure, the atoms equivalent to N2 and N5 in (I) have significant sp^2 character based on the sums of the angles about these atoms. This is also true in (I) where the angles sum to 360.2 and 359.2°, respectively. The same considerations led the authors to conclude that the N3 and N6 atoms have some sp^3 character. Substantiating this conclusion, in (I) the sum of the angles amount to 344.0 and 346.4°, respectively. Finally, the C1—N2 and C14—N5 bond lengths of 1.334 (7) and 1.365 (8) Å, respectively, are indicative of some double-bond character, an observation again consistent with the literature precedent.

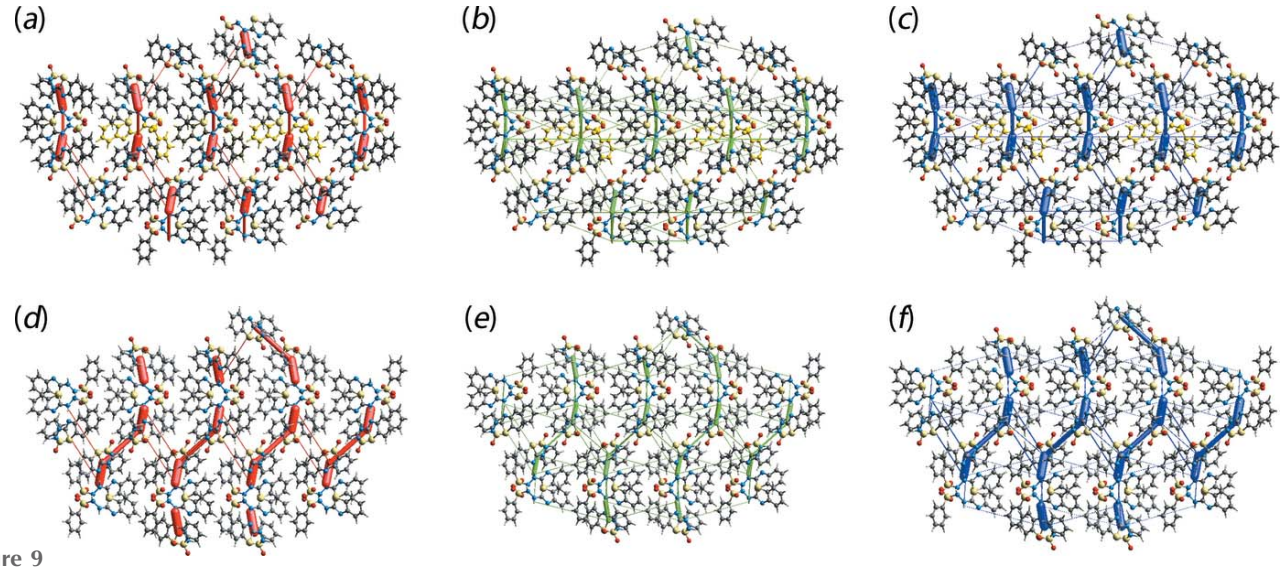

Figure 9
A comparison of the energy frameworks composed of (*a*) electrostatic potential force, (*b*) dispersion force and (*c*) total energy for for the S1-molecule and and (*d*)–(*f*) comparable frameworks for the S3-molecule. The energy frameworks were adjusted to the same scale factor of 50 with a cut-off value of 5 kJ mol^{-1} within 2 × 2 × 2 unit cells.

7. Synthesis and crystallization

The melting point was determined on a Griffin melting point apparatus and is uncorrected. Infrared spectra, as neat powders, were recorded using a Perkin Elmer UATR two instrument, with an ATR Diamond Cell NMR spectra were recorded on a Bruker Avance 400 spectrometer in DMSO-d_6 solution at room temperature. Accurate mass measurements were determined using a Water Mass Spectrometer Model Xevo G2 QT instrument.

Preparation: A solution of 2-hydrazinyl-1,3-benzothiazole (1.66 g, 1 mmol) and benzenesulfonyl chloride (1.77 g, 1 mmol) in EtOAc (20 ml) was refluxed for 1 h. The reaction mixture was washed with water, the organic layer was collected, dried over magnesium sulfate and rotary evaporated. The residue was recrystallized from an ethanol solution. Yield 82%. The sample used in the structure determination was obtained by slow evaporation of an ethanol solution at room temperature after two days; m.p. 643–465 K. IR (cm^{-1}): 3202, 3100–2600 (*br*), 1615, 1583, 1466, 1448, 1325, 1274 1161, 1087, 888, 746, 637. ^{1}H NMR (400 MHz, DMSO-d_6): δ 7.15(1H, *t*), 7.31(1H, *br*), 7.40(1H, *br. s*), 7.67(2H, *t*), 7.78(2H, *m*), 7.94(2H, *d*); NH not observed. ^{13}C{^{1}H} NMR (100 MHz, DMSO-d_6): δ 121.91, 122.22, 125.96, 126.34, 128.24, 128.85, 129.67, 133.81, 138.67, 171.78. Accurate mass: found [M + H] = 306.0370; calculated 306.0371.

8. Refinement details

Crystal data, data collection and structure refinement details are summarized in Table 6. The carbon-bound H atoms were placed in calculated positions (C—H = 0.95 Å) and were included in the refinement in the riding-model approximation, with U_{iso}(H) set to 1.2–1.5U_{eq}(C). The N-bound H atoms were refined with a distance restraint of 0.88±0.01 Å, and with U_{iso}(H) = 1.2U_{eq}(N). Owing to poor agreement, two reflections, *i.e.* (1 5 11) and (1 7 15), were omitted from the final cycles of refinement.

Table 6
Experimental details.

Crystal data	
Chemical formula	$C_{13}H_{11}N_3O_2S_2$
M_r	305.37
Crystal system, space group	Orthorhombic, *Pbca*
Temperature (K)	100
a, *b*, *c* (Å)	8.9083 (7), 21.6499 (9), 29.4778 (18)
V (Å^3)	5685.2 (6)
Z	16
Radiation type	Synchrotron, λ = 0.6889 Å
μ (mm^{-1})	0.34
Crystal size (mm)	0.01 × 0.01 × 0.01
Data collection	
Diffractometer	Three-circle diffractometer
Absorption correction	Empirical (using intensity measurements) (*AIMLESS CCP4*; Evans, 2006)
T_{min}, T_{max}	0.996, 1.000
No. of measured, independent and observed [$I > 2\sigma(I)$] reflections	15484, 5451, 2289
R_{int}	0.199
(sin $\theta/\lambda)_{max}$ (Å^{-1})	0.613
Refinement	
$R[F^2 > 2\sigma(F^2)]$, $wR(F^2)$, S	0.083, 0.246, 0.77
No. of reflections	5451
No. of parameters	373
No. of restraints	4
H-atom treatment	H atoms treated by a mixture of independent and constrained refinement
$\Delta\rho_{max}$, $\Delta\rho_{min}$ (e Å^{-3})	0.56, −0.44

Computer programs: *GDA* (http://www.opengda.org/OpenGDA.html), *XIA2 0.4.0.370-g47f3bc3* (Winter, 2010), *SHELXS97* (Sheldrick, 2008), *SHELXL2018* (Sheldrick, 2015), *ORTEP-3 for Windows* (Farrugia, 2012), *Q-Mol* Gans & Shalloway (2001) and *DIAMOND* (Brandenburg, 2006) and *publCIF* (Westrip, 2010).

Acknowledgements

We thank the EPSRC National Crystallography Service (University of Southampton) for the X-ray data collections.

References

Brandenburg, K. (2006). *DIAMOND*. Crystal Impact GbR, Bonn, Germany.
Dar, A. A., Shadab, M., Khan, S., Ali, N. & Khan, A. T. (2016). *J. Org. Chem.* **81**, 3149–3160.
Evans, P. (2006). *Acta Cryst.* D**62**, 72–82.
Farrugia, L. J. (2012). *J. Appl. Cryst.* **45**, 849–854.
Gans, J. & Shalloway, D. (2001). *J. Mol. Graph. Model.* **19**, 557–559.
Gill, R. K., Rawal, R. K. & Bariwal, J. (2015). *Arch. Pharm. Chem. Life Sci.* **348**, 155–178.
Katava, R., Pavelić, S. K., Harej, A., Hrenar, T. & Pavlović, G. (2017). *Struct. Chem.* **28**, 709–721.
Lindgren, E. B., de Brito, M. A., Vasconcelos, T. R. A., de Moraes, M. O., Montenegro, R. C., Yoneda, J. D. & Leal, K. Z. (2014). *Eur. J. Med. Chem.* **86**, 12–16.
Morscher, A., de Souza, M. V. N., Wardell, J. L. & Harrison, W. T. A. (2018). *Acta Cryst.* E**74**, 673–677.
Nogueira, A. F., Azevedo, E. C., Ferreira, V. F., Araújo, A. J., Santos, E. A., Pessoa, C., Costa-Lotufo, L. V., Montenegro, R. C., Moraes, M. O. & Vasconcelos, T. R. A. (2010). *Lett. Drug. Des. Discov.* **7**, 551–555.
Pinheiro, A. C., de Souza, M. V. N., Lourenço, M. C. S., da Costa, C. F., Baddeley, T. C., Low, J. N., Wardell, S. M. S. V. & Wardell, J. L. (2019). *J. Mol. Struct.* **1178**, 655–668.
Rao, D. S., Jayachandran, E., Srinivasa, G. M. & Shivakumar, B. (2004). *Indian J. Heterocycl. Chem.* **14**, 65–66.
Reshma, R. S., Jeankumar, V. U., Kapoor, N., Saxena, S., Bobesh, K. A., Vachaspathy, A. R., Kolattukudy, P. E. & Sriram, D. (2017). *Bioorg. Med. Chem.* **25**, 2761–2771.
Sheldrick, G. M. (2008). *Acta Cryst.* A**64**, 112–122.
Sheldrick, G. M. (2015). *Acta Cryst.* C**71**, 3–8.
Spek, A. L. (2009). *Acta Cryst.* D**65**, 148–155.
Tan, S. L., Jotani, M. M. & Tiekink, E. R. T. (2019). *Acta Cryst.* E**75**, 308–318.
Thakkar, S. S., Thakor, P., Ray, A., Doshi, H. & Thakkar, V. R. (2017). *Bioorg. Med. Chem.* **25**, 5396–5406.
Turner, M. J., Mckinnon, J. J., Wolff, S. K., Grimwood, D. J., Spackman, P. R., Jayatilaka, D. & Spackman, M. A. (2017). *Crystal Explorer 17*. The University of Western Australia.
Westrip, S. P. (2010). *J. Appl. Cryst.* **43**, 920–925.
Winter, G. (2010). *J. Appl. Cryst.* **43**, 186–190.

supporting information

Acta Cryst. (2019). E**75**, 516-523 [https://doi.org/10.1107/S2056989019003980]

N′-(1,3-Benzothiazol-2-yl)benzenesulfonohydrazide: crystal structure, Hirshfeld surface analysis and computational chemistry

Thomas C. Baddeley, Marcus V. N. de Souza, James L. Wardell, Mukesh M. Jotani and Edward R. T. Tiekink

Computing details

Data collection: *GDA* (http://www.opengda.org/OpenGDA.html); cell refinement: *XIA2 0.4.0.370-g47f3bc3* (Winter, 2010); data reduction: *XIA2 0.4.0.370-g47f3bc3* (Winter, 2010); program(s) used to solve structure: *SHELXS97* (Sheldrick, 2008); program(s) used to refine structure: *SHELXL2018* (Sheldrick, 2015); molecular graphics: *ORTEP-3 for Windows* (Farrugia, 2012), *Q-Mol* Gans & Shalloway (2001) and *DIAMOND* (Brandenburg, 2006); software used to prepare material for publication: *publCIF* (Westrip, 2010).

N′-(1,3-Benzothiazol-2-yl)benzenesulfonohydrazide

Crystal data

$C_{13}H_{11}N_3O_2S_2$
M_r = 305.37
Orthorhombic, *Pbca*
a = 8.9083 (7) Å
b = 21.6499 (9) Å
c = 29.4778 (18) Å
V = 5685.2 (6) Å^3
Z = 16
F(000) = 2528
D_x = 1.427 Mg m^{-3}
Synchrotron radiation, λ = 0.6889 Å
Cell parameters from 2386 reflections
θ = 2.5–28.6°
μ = 0.34 mm^{-1}
T = 100 K
Cube, colourless
0.01 × 0.01 × 0.01 mm

Data collection

Three-circle diffractometer
Radiation source: synchrotron, DLS beamline I19, undulator
Si 111, double crystal monochromator
Detector resolution: 5.81 pixels mm^{-1}
profile data from ω–scans
Absorption correction: empirical (using intensity measurements) (*AIMLESS CCP4*; Evans, 2006)
T_{min} = 0.996, T_{max} = 1.000
15484 measured reflections
5451 independent reflections
2289 reflections with $I > 2\sigma(I)$
R_{int} = 0.199
θ_{max} = 25.0°, θ_{min} = 1.8°
h = −10→10
k = −10→26
l = −31→35

Refinement

Refinement on F^2
Least-squares matrix: full
$R[F^2 > 2\sigma(F^2)]$ = 0.083
$wR(F^2)$ = 0.246
S = 0.77
5451 reflections
373 parameters
4 restraints
Primary atom site location: structure-invariant direct methods

Secondary atom site location: difference Fourier map	$w = 1/[\sigma^2(F_o^2) + (0.1P)^2]$ where $P = (F_o^2 + 2F_c^2)/3$
Hydrogen site location: mixed	$(\Delta/\sigma)_{max} = 0.001$
H atoms treated by a mixture of independent and constrained refinement	$\Delta\rho_{max} = 0.56$ e Å^{-3}
	$\Delta\rho_{min} = -0.44$ e Å^{-3}

Special details

Geometry. All esds (except the esd in the dihedral angle between two l.s. planes) are estimated using the full covariance matrix. The cell esds are taken into account individually in the estimation of esds in distances, angles and torsion angles; correlations between esds in cell parameters are only used when they are defined by crystal symmetry. An approximate (isotropic) treatment of cell esds is used for estimating esds involving l.s. planes.

Refinement. The sample was small and data were measured on the DLS beamline I19 with synchrotron radiation. The crystal dimensions were not recorded and assumed to be 0.01 x 0.01 x 0.01 mm^3. Data were truncated at $\theta = 25.0$ so data completeness was > 99%. The value of R_{int} is high but, the ordered structure has been determined unambiguously. The GoF is poor but, this probably reflects the limited data available for the sample investigated.

Fractional atomic coordinates and isotropic or equivalent isotropic displacement parameters (Å²)

	x	*y*	*z*	U_{iso}*/U_{eq}
S1	0.60554 (19)	0.58255 (6)	0.24704 (5)	0.0503 (4)
S2	0.51420 (19)	0.75258 (5)	0.27917 (5)	0.0454 (4)
O1	0.6648 (5)	0.73163 (18)	0.28878 (14)	0.0592 (12)
O2	0.4882 (6)	0.79329 (17)	0.24171 (13)	0.0646 (13)
N1	0.5102 (6)	0.55146 (19)	0.32861 (15)	0.0514 (13)
N2	0.4129 (6)	0.64482 (19)	0.30137 (16)	0.0481 (12)
H2N	0.353 (6)	0.645 (3)	0.3252 (13)	0.058*
N3	0.4169 (6)	0.68926 (18)	0.26694 (16)	0.0440 (12)
H3N	0.329 (3)	0.695 (3)	0.2542 (18)	0.053*
C1	0.4979 (7)	0.5945 (2)	0.29675 (19)	0.0482 (15)
C2	0.6739 (7)	0.5141 (2)	0.2705 (2)	0.0513 (15)
C3	0.7784 (8)	0.4730 (2)	0.2528 (2)	0.0598 (18)
H3	0.819254	0.478886	0.223372	0.072*
C4	0.8222 (9)	0.4221 (3)	0.2800 (3)	0.075 (2)
H4	0.896758	0.394257	0.269346	0.090*
C5	0.7563 (9)	0.4127 (2)	0.3222 (3)	0.071 (2)
H5	0.784616	0.377377	0.339315	0.085*
C6	0.6517 (9)	0.4526 (3)	0.3401 (2)	0.0657 (19)
H6	0.608183	0.445225	0.369067	0.079*
C7	0.6109 (7)	0.5049 (2)	0.3141 (2)	0.0548 (17)
C8	0.4406 (7)	0.7849 (2)	0.32924 (17)	0.0452 (15)
C9	0.4975 (9)	0.7651 (3)	0.3714 (2)	0.0587 (18)
H9	0.576259	0.735541	0.372649	0.070*
C10	0.4387 (13)	0.7887 (4)	0.4107 (2)	0.093 (3)
H10	0.476103	0.775303	0.439199	0.111*
C11	0.3247 (15)	0.8321 (5)	0.4089 (4)	0.114 (4)
H11	0.284576	0.848228	0.436261	0.137*
C12	0.2685 (11)	0.8522 (3)	0.3677 (4)	0.095 (3)
H12	0.190565	0.882071	0.366926	0.114*
C13	0.3267 (8)	0.8284 (3)	0.3273 (2)	0.0628 (18)

H13	0.288543	0.841850	0.298885	0.075*
S3	0.2032 (2)	0.65517 (7)	0.46859 (5)	0.0588 (5)
S4	0.6181 (2)	0.59193 (6)	0.47670 (6)	0.0584 (5)
O3	0.6133 (6)	0.65715 (17)	0.47139 (16)	0.0706 (14)
O4	0.6304 (6)	0.56392 (19)	0.52128 (14)	0.0711 (14)
N4	0.2271 (6)	0.65127 (19)	0.37953 (16)	0.0492 (13)
N5	0.3982 (7)	0.5865 (2)	0.41732 (17)	0.0651 (16)
H5N	0.431 (8)	0.569 (3)	0.3921 (13)	0.078*
N6	0.4514 (7)	0.5658 (2)	0.45953 (17)	0.0601 (15)
H6N	0.431 (8)	0.5261 (9)	0.464 (2)	0.072*
C14	0.2839 (8)	0.6284 (2)	0.4175 (2)	0.0534 (16)
C15	0.0812 (8)	0.7021 (3)	0.4356 (2)	0.0546 (16)
C16	−0.0275 (8)	0.7435 (2)	0.4501 (2)	0.0553 (16)
H16	−0.045765	0.749907	0.481528	0.066*
C17	−0.1100 (8)	0.7757 (3)	0.4169 (2)	0.0606 (18)
H17	−0.186125	0.803973	0.425736	0.073*
C18	−0.0795 (9)	0.7660 (3)	0.3712 (2)	0.0596 (18)
H18	−0.136054	0.787920	0.349092	0.072*
C19	0.0311 (8)	0.7252 (2)	0.3567 (2)	0.0524 (16)
H19	0.050144	0.719456	0.325307	0.063*
C20	0.1132 (7)	0.6931 (2)	0.38891 (19)	0.0479 (15)
C21	0.7612 (8)	0.5609 (3)	0.4423 (2)	0.0597 (18)
C22	0.8006 (10)	0.5918 (3)	0.4026 (3)	0.075 (2)
H22	0.753526	0.629700	0.394779	0.090*
C23	0.9117 (10)	0.5660 (4)	0.3740 (3)	0.086 (3)
H23	0.936312	0.585303	0.345993	0.103*
C24	0.9838 (11)	0.5125 (4)	0.3871 (4)	0.101 (3)
H24	1.059314	0.495490	0.368104	0.122*
C25	0.9477 (11)	0.4826 (4)	0.4283 (3)	0.095 (3)
H25	1.000034	0.446322	0.437183	0.114*
C26	0.8351 (9)	0.5066 (3)	0.4555 (3)	0.074 (2)
H26	0.808163	0.486493	0.483000	0.089*

Atomic displacement parameters (Å²)

	U^{11}	U^{22}	U^{33}	U^{12}	U^{13}	U^{23}
S1	0.0531 (11)	0.0425 (7)	0.0551 (9)	−0.0019 (6)	0.0039 (7)	−0.0034 (6)
S2	0.0498 (11)	0.0427 (7)	0.0438 (8)	−0.0055 (6)	0.0029 (7)	−0.0036 (6)
O1	0.048 (3)	0.061 (2)	0.068 (3)	0.004 (2)	0.000 (2)	−0.020 (2)
O2	0.097 (4)	0.053 (2)	0.044 (2)	−0.019 (2)	0.005 (2)	0.0073 (17)
N1	0.060 (4)	0.042 (2)	0.053 (3)	0.004 (2)	0.001 (2)	−0.004 (2)
N2	0.049 (4)	0.044 (2)	0.051 (3)	0.004 (2)	0.007 (2)	0.009 (2)
N3	0.047 (3)	0.036 (2)	0.049 (3)	0.002 (2)	−0.003 (2)	0.0000 (18)
C1	0.049 (4)	0.038 (3)	0.058 (4)	−0.002 (2)	−0.003 (3)	−0.005 (2)
C2	0.042 (4)	0.041 (3)	0.071 (4)	−0.006 (2)	0.003 (3)	−0.007 (3)
C3	0.061 (5)	0.037 (3)	0.081 (5)	−0.006 (3)	0.005 (4)	−0.011 (3)
C4	0.069 (6)	0.040 (3)	0.118 (7)	0.000 (3)	0.012 (5)	−0.019 (3)
C5	0.076 (6)	0.039 (3)	0.097 (6)	0.009 (3)	−0.006 (4)	−0.001 (3)

C6	0.079 (6)	0.047 (3)	0.071 (4)	0.003 (3)	0.000 (4)	0.001 (3)
C7	0.059 (5)	0.038 (3)	0.067 (4)	−0.001 (3)	−0.007 (3)	−0.007 (3)
C8	0.064 (5)	0.033 (2)	0.039 (3)	−0.009 (3)	0.014 (3)	−0.003 (2)
C9	0.076 (6)	0.053 (3)	0.047 (4)	−0.013 (3)	0.007 (3)	0.000 (3)
C10	0.143 (9)	0.091 (5)	0.045 (4)	−0.047 (6)	0.019 (5)	−0.025 (4)
C11	0.139 (10)	0.105 (7)	0.098 (7)	−0.072 (7)	0.075 (7)	−0.058 (6)
C12	0.080 (7)	0.059 (4)	0.146 (9)	−0.010 (4)	0.042 (6)	−0.043 (5)
C13	0.051 (5)	0.049 (3)	0.088 (5)	0.003 (3)	0.005 (4)	−0.008 (3)
S3	0.0749 (14)	0.0598 (8)	0.0417 (9)	0.0072 (8)	−0.0022 (8)	0.0074 (6)
S4	0.0721 (14)	0.0445 (7)	0.0587 (10)	0.0039 (7)	−0.0046 (9)	−0.0027 (6)
O3	0.085 (4)	0.045 (2)	0.082 (3)	−0.005 (2)	0.013 (3)	0.002 (2)
O4	0.095 (4)	0.060 (2)	0.058 (3)	0.005 (2)	−0.008 (2)	−0.005 (2)
N4	0.058 (4)	0.046 (2)	0.044 (3)	−0.003 (2)	0.001 (2)	0.007 (2)
N5	0.087 (5)	0.070 (3)	0.038 (3)	0.026 (3)	−0.003 (3)	0.009 (2)
N6	0.081 (5)	0.043 (2)	0.056 (3)	−0.001 (3)	−0.003 (3)	0.010 (2)
C14	0.062 (5)	0.045 (3)	0.053 (4)	−0.003 (3)	0.003 (3)	0.002 (3)
C15	0.064 (5)	0.057 (3)	0.042 (3)	−0.007 (3)	−0.007 (3)	0.004 (3)
C16	0.060 (5)	0.058 (3)	0.048 (4)	0.002 (3)	0.001 (3)	0.002 (3)
C17	0.064 (5)	0.056 (3)	0.062 (4)	0.011 (3)	−0.006 (3)	−0.002 (3)
C18	0.075 (6)	0.062 (3)	0.041 (3)	0.016 (3)	−0.005 (3)	−0.001 (3)
C19	0.067 (5)	0.048 (3)	0.042 (3)	−0.006 (3)	0.000 (3)	0.006 (2)
C20	0.046 (4)	0.050 (3)	0.048 (4)	−0.011 (3)	−0.001 (3)	0.008 (2)
C21	0.068 (5)	0.052 (3)	0.060 (4)	−0.007 (3)	−0.003 (3)	−0.003 (3)
C22	0.091 (7)	0.053 (3)	0.082 (5)	−0.019 (4)	0.007 (5)	−0.012 (3)
C23	0.099 (7)	0.071 (5)	0.088 (6)	−0.036 (5)	0.022 (5)	−0.029 (4)
C24	0.068 (7)	0.098 (6)	0.139 (9)	−0.015 (5)	0.024 (6)	−0.053 (6)
C25	0.081 (7)	0.076 (5)	0.127 (8)	0.011 (4)	0.010 (6)	−0.023 (5)
C26	0.070 (6)	0.065 (4)	0.087 (5)	0.015 (4)	0.003 (4)	−0.013 (4)

Geometric parameters (Å, º)

S1—C2	1.746 (6)	S3—C14	1.766 (6)
S1—C1	1.770 (6)	S3—C15	1.777 (6)
S2—O2	1.432 (4)	S4—O3	1.421 (4)
S2—O1	1.444 (5)	S4—O4	1.451 (5)
S2—N3	1.662 (5)	S4—N6	1.668 (6)
S2—C8	1.760 (5)	S4—C21	1.761 (7)
N1—C1	1.327 (7)	N4—C14	1.325 (7)
N1—C7	1.416 (7)	N4—C20	1.388 (8)
N2—C1	1.334 (7)	N5—C14	1.365 (8)
N2—N3	1.399 (6)	N5—N6	1.405 (7)
N2—H2N	0.880 (10)	N5—H5N	0.884 (10)
N3—H3N	0.877 (10)	N6—H6N	0.886 (10)
C2—C3	1.389 (9)	C15—C16	1.387 (9)
C2—C7	1.415 (9)	C15—C20	1.419 (8)
C3—C4	1.418 (9)	C16—C17	1.409 (9)
C3—H3	0.9500	C16—H16	0.9500
C4—C5	1.390 (10)	C17—C18	1.392 (9)

C4—H4	0.9500	C17—H17	0.9500
C5—C6	1.376 (10)	C18—C19	1.389 (9)
C5—H5	0.9500	C18—H18	0.9500
C6—C7	1.416 (8)	C19—C20	1.384 (8)
C6—H6	0.9500	C19—H19	0.9500
C8—C13	1.386 (9)	C21—C22	1.394 (9)
C8—C9	1.410 (8)	C21—C26	1.402 (9)
C9—C10	1.369 (10)	C22—C23	1.415 (11)
C9—H9	0.9500	C22—H22	0.9500
C10—C11	1.383 (15)	C23—C24	1.380 (12)
C10—H10	0.9500	C23—H23	0.9500
C11—C12	1.382 (14)	C24—C25	1.413 (13)
C11—H11	0.9500	C24—H24	0.9500
C12—C13	1.397 (11)	C25—C26	1.387 (11)
C12—H12	0.9500	C25—H25	0.9500
C13—H13	0.9500	C26—H26	0.9500

C2—S1—C1	89.1 (3)	C14—S3—C15	88.3 (3)
O2—S2—O1	119.7 (3)	O3—S4—O4	121.1 (3)
O2—S2—N3	104.8 (2)	O3—S4—N6	106.1 (3)
O1—S2—N3	105.5 (2)	O4—S4—N6	101.5 (3)
O2—S2—C8	110.0 (3)	O3—S4—C21	109.7 (3)
O1—S2—C8	107.8 (3)	O4—S4—C21	107.9 (3)
N3—S2—C8	108.4 (3)	N6—S4—C21	109.9 (3)
C1—N1—C7	109.7 (5)	C14—N4—C20	110.8 (5)
C1—N2—N3	118.2 (5)	C14—N5—N6	117.4 (5)
C1—N2—H2N	116 (4)	C14—N5—H5N	122 (5)
N3—N2—H2N	126 (4)	N6—N5—H5N	120 (5)
N2—N3—S2	115.0 (4)	N5—N6—S4	117.4 (4)
N2—N3—H3N	112 (4)	N5—N6—H6N	111 (4)
S2—N3—H3N	117 (4)	S4—N6—H6N	118 (5)
N1—C1—N2	123.2 (5)	N4—C14—N5	122.0 (5)
N1—C1—S1	116.0 (4)	N4—C14—S3	116.3 (5)
N2—C1—S1	120.7 (4)	N5—C14—S3	121.7 (4)
C3—C2—C7	121.1 (5)	C16—C15—C20	121.9 (6)
C3—C2—S1	128.9 (5)	C16—C15—S3	128.9 (5)
C7—C2—S1	109.9 (4)	C20—C15—S3	109.3 (5)
C2—C3—C4	118.0 (6)	C15—C16—C17	118.0 (6)
C2—C3—H3	121.0	C15—C16—H16	121.0
C4—C3—H3	121.0	C17—C16—H16	121.0
C5—C4—C3	120.2 (6)	C18—C17—C16	119.8 (6)
C5—C4—H4	119.9	C18—C17—H17	120.1
C3—C4—H4	119.9	C16—C17—H17	120.1
C6—C5—C4	122.6 (6)	C19—C18—C17	122.1 (6)
C6—C5—H5	118.7	C19—C18—H18	119.0
C4—C5—H5	118.7	C17—C18—H18	119.0
C5—C6—C7	117.8 (6)	C20—C19—C18	118.9 (6)
C5—C6—H6	121.1	C20—C19—H19	120.5

C7—C6—H6	121.1	C18—C19—H19	120.5
N1—C7—C6	124.6 (6)	C19—C20—N4	125.2 (5)
N1—C7—C2	115.2 (5)	C19—C20—C15	119.3 (6)
C6—C7—C2	120.2 (6)	N4—C20—C15	115.4 (5)
C13—C8—C9	120.4 (6)	C22—C21—C26	121.2 (7)
C13—C8—S2	120.6 (5)	C22—C21—S4	118.9 (5)
C9—C8—S2	119.0 (5)	C26—C21—S4	119.9 (5)
C10—C9—C8	119.6 (8)	C21—C22—C23	119.2 (7)
C10—C9—H9	120.2	C21—C22—H22	120.4
C8—C9—H9	120.2	C23—C22—H22	120.4
C9—C10—C11	120.1 (8)	C24—C23—C22	119.3 (8)
C9—C10—H10	119.9	C24—C23—H23	120.4
C11—C10—H10	119.9	C22—C23—H23	120.4
C12—C11—C10	120.9 (7)	C23—C24—C25	121.4 (8)
C12—C11—H11	119.6	C23—C24—H24	119.3
C10—C11—H11	119.6	C25—C24—H24	119.3
C11—C12—C13	119.9 (8)	C26—C25—C24	119.3 (8)
C11—C12—H12	120.1	C26—C25—H25	120.3
C13—C12—H12	120.1	C24—C25—H25	120.3
C8—C13—C12	119.1 (7)	C25—C26—C21	119.5 (8)
C8—C13—H13	120.4	C25—C26—H26	120.2
C12—C13—H13	120.4	C21—C26—H26	120.2

C1—N2—N3—S2	−104.5 (5)	C14—N5—N6—S4	−106.6 (6)
O2—S2—N3—N2	−173.6 (4)	O3—S4—N6—N5	49.7 (5)
O1—S2—N3—N2	59.1 (4)	O4—S4—N6—N5	177.1 (4)
C8—S2—N3—N2	−56.2 (5)	C21—S4—N6—N5	−68.8 (5)
C7—N1—C1—N2	−178.6 (5)	C20—N4—C14—N5	−179.6 (6)
C7—N1—C1—S1	0.1 (6)	C20—N4—C14—S3	0.5 (7)
N3—N2—C1—N1	175.5 (5)	N6—N5—C14—N4	179.2 (5)
N3—N2—C1—S1	−3.1 (7)	N6—N5—C14—S3	−0.9 (8)
C2—S1—C1—N1	−0.1 (5)	C15—S3—C14—N4	−0.3 (5)
C2—S1—C1—N2	178.6 (5)	C15—S3—C14—N5	179.9 (6)
C1—S1—C2—C3	−177.5 (6)	C14—S3—C15—C16	−178.1 (6)
C1—S1—C2—C7	0.1 (5)	C14—S3—C15—C20	−0.1 (4)
C7—C2—C3—C4	−1.1 (9)	C20—C15—C16—C17	1.9 (9)
S1—C2—C3—C4	176.3 (5)	S3—C15—C16—C17	179.7 (5)
C2—C3—C4—C5	2.8 (10)	C15—C16—C17—C18	−0.9 (10)
C3—C4—C5—C6	−2.4 (11)	C16—C17—C18—C19	−0.2 (10)
C4—C5—C6—C7	0.0 (11)	C17—C18—C19—C20	0.2 (10)
C1—N1—C7—C6	178.9 (6)	C18—C19—C20—N4	−179.7 (6)
C1—N1—C7—C2	0.0 (7)	C18—C19—C20—C15	0.8 (9)
C5—C6—C7—N1	−177.1 (6)	C14—N4—C20—C19	179.9 (6)
C5—C6—C7—C2	1.7 (10)	C14—N4—C20—C15	−0.6 (7)
C3—C2—C7—N1	177.7 (6)	C16—C15—C20—C19	−1.8 (9)
S1—C2—C7—N1	−0.1 (7)	S3—C15—C20—C19	180.0 (5)
C3—C2—C7—C6	−1.2 (9)	C16—C15—C20—N4	178.6 (6)
S1—C2—C7—C6	−179.0 (5)	S3—C15—C20—N4	0.4 (6)

O2—S2—C8—C13	23.5 (6)	O3—S4—C21—C22	−28.5 (7)
O1—S2—C8—C13	155.6 (5)	O4—S4—C21—C22	−162.4 (5)
N3—S2—C8—C13	−90.6 (5)	N6—S4—C21—C22	87.8 (6)
O2—S2—C8—C9	−157.6 (5)	O3—S4—C21—C26	150.3 (6)
O1—S2—C8—C9	−25.5 (5)	O4—S4—C21—C26	16.5 (7)
N3—S2—C8—C9	88.3 (5)	N6—S4—C21—C26	−93.4 (6)
C13—C8—C9—C10	0.5 (9)	C26—C21—C22—C23	3.4 (11)
S2—C8—C9—C10	−178.3 (5)	S4—C21—C22—C23	−177.8 (6)
C8—C9—C10—C11	−0.4 (11)	C21—C22—C23—C24	−3.2 (11)
C9—C10—C11—C12	0.1 (13)	C22—C23—C24—C25	0.8 (12)
C10—C11—C12—C13	0.3 (13)	C23—C24—C25—C26	1.5 (13)
C9—C8—C13—C12	−0.2 (9)	C24—C25—C26—C21	−1.3 (13)
S2—C8—C13—C12	178.6 (5)	C22—C21—C26—C25	−1.1 (11)
C11—C12—C13—C8	−0.2 (11)	S4—C21—C26—C25	−179.9 (6)

Hydrogen-bond geometry (Å, º)

D—H···*A*	*D*—H	H···*A*	*D*···*A*	*D*—H···*A*
N2—H2*N*···N4	0.88 (4)	1.96 (4)	2.840 (7)	176 (8)
N3—H3*N*···O1^{i}	0.88 (3)	2.09 (4)	2.930 (7)	160 (5)
N5—H5*N*···N1	0.88 (5)	2.04 (4)	2.900 (7)	165 (6)
N6—H6*N*···O4^{ii}	0.89 (3)	2.07 (3)	2.956 (6)	175 (6)
C4—H4···O2^{iii}	0.95	2.55	3.450 (8)	159

Symmetry codes: (i) *x*−1/2, *y*, −*z*+1/2; (ii) −*x*+1, −*y*+1, −*z*+1; (iii) −*x*+3/2, *y*−1/2, *z*.